DOE/PC/70029--T9

Project Status Report

Mechanism of Promotion of Iron Fischer-Tropsch Catalysts (Quarterly Report for the Period Ending March 31, 1986)

Contract No.: DE-AC22-84PC70029

Contractor: University of Louisville Research Foundation
University of Louisville
Graduate Programs and Research
Louisville, KY 40292

Contract Starting Date: September 27, 1984

Contract Completion Date: September 26, 1987

DOE/PC/70029--T9

DE89 010832

SUMMARY

^{14}C labeled ethanol, when added to a CO/H_2 feed, undergoes dehydrogenation to establish essentially an equilibrium ethanol-acetaldehyde mixture. ^{14}C ethanol also incorporates to form higher carbon number alcohols and hydrocarbons. However, under the reaction conditions used, ethyl acetate and 1,1-diethoxyethane (actual) are significant products; the ^{14}C label permits us to identify these products as being derived from ethanol. In addition, it appears that aldol condensation of acetaldehyde occurs to a minor extent. In brief, there appear to be significant differences between the current results with a $Fe-SiO_2$ catalyst and the earlier results with promoted iron catalysts; subsequent investigations will define these differences.

The time required to attain a steady-state concentration of ^{14}C labeled, or unlabeled, ethanol in a CO/H_2 reactor effluent is much longer than the anticipated 15 minutes following the initiation of ethanol addition to a syngas feed. Evidence is presented to support the view that ethanol solubility in the wax present in the stirred autoclave reactor retards

---

attainment of the equiliberation. Data with ^{14}C labeled pentanol and decanol support this view. This result, if confirmed, supports the view of accumulation of products, and concurrent secondary reactions, that depends upon both carbon number and compound class.

INTRODUCTION

Oxygen containing compounds are found in Fischer-Tropsch Synthesis products when iron catalysts are employed. These oxygen containing products have received much attention since the pioneering work of Emmett and coworkers (1-8). The results from a series of isotope labeling studies clearly showed that alcohols could serve as chain initiations for the polymerization reactions. Emmett, to carry out his studies, had to resort to gross separation by distillation and to obtain an "average" hydrocarbon composition and ^{14}C label. High resolution gas and liquid chromatographic techniques were unavailable to Emmett and coworkers and it is truly amazing that they were able to accomplish as much as they did. Schulz and coworkers (9-13) have confirmed, and extended, many of the ^{14}C isotope labeling results obtained by Emmett and coworkers. However, these workers did not report the details of the oxygenates formed when alcohols are added to a syngas feed.

EXPERIMENTAL

An experimental system consisting of gas flow regulators, a 1 liter stirred autoclave reactor, hot and cold product traps and in-line g.c. for gas stream analysis. The catalyst contained 9.2% Fe that was prepared by adding aqueous ferric nitrate to a Davison 923 silica gel using an incipient wetness technique. The impregnated silica was dried at 120°C and then calcined at 450°C for 4 hours. The material (120 grams) was reduced for 24 hours at 450°C in ca. 100 cc/min. hydrogen flow; the reduced catalyst was then charged to the stirred autoclave reactor. Approximately 500 cc of n-octacosane, purified by recrystallization from THF, was added to the reactor and the catalyst rereduced in-situ. Synthesis runs were carried out 265°C, 90 psig, CO/H_2 ratio of 0.78, 5cc/sec. syngas flow, and 600 rpm reactor stirrer speed. ^{14}C labeled alcohol was pumped into the heated (ca. 100°C) syngas stream immediately prior to entering the reactor; the pump rate was adjusted to provide 3 volume % ^{14}C label (based on CO, not total gas flow). Liquid products were collected in hot (ca. 60°C) or cold (ca. 5°C) traps. Gas passing through the cold trap was sampled and analyzed by one of two g.c.'s: (1) A Carle valve g.c. (Hacks) using a combination of six columns to effect analysis of CO, H_2, CO_2 and all the hydrocarbons below C_5, and (2) a 6 ft. 1/8" Porpack R column (Supelco) to obtain analysis of C_5^+ hydrocarbons. Thermal conductivity g.c. detectors were used so that the g.c. effluent could be passed through a short heat-traced line directly to a Packard Model 894 gas proportional counter. Prior to ^{14}C detection each effluent peak was burned to CO_2 and mixed with methane quench gas.

Gas chromatographic-mass spectrometric analyses were performed on a Hewlett-Packard 5985A capillary gc/quadrupole mass spectrometer system. GC

separation was carried out on an OV1 WCOT column and mass spectra were recorded every 2 seconds. The spectrometer was operated in the EI mode at 70V electron energy and a source temperature of 150°C. Component identification was aided by search of a mass spectral library.

The g.c.-i.r. analytical method utilized a matrix isolation (MI) interface (Cryolect, Matheson Instruments) with a Varian 3700 capillary g.c. and a Sirus FTIR. A 10% split of the gas eluting from a capillary column (DB-5) was mixed with Ar and diverted to a slowly turning circular disc which had a gold mirror plating on the circumference. The peaks, in the order they elute from the g.c. column, are condensed in an Ar matrix on the circumference of the disc. Each peak is deposited at a unique location as the disc turns; a computer maintains a log of the location of a condensed peak upon the disc by retention time and disc revolution speed. At the completion of a chromatogram, the disc may be repositioned to obtain an i.r. spectrum of the component(s) of the desired peaks that were condensed in Ar.

RESULTS

Results for the paraffin product distribution, defined as % paraffin C_m = C_m total n-alkane + n-alkene products, are presented in Figure 1 for (a) CO/H_2 syngas feed only (■) and CO/H_2 syngas with added ethanol (□). The product distributions are similar for the two runs; however, slightly more olefins are formed when the alcohol was added to the feed.

Several oxygenated products were formed from ethanol (Table 1). Possible pathways for these products are outlined below:

$$C_2H_5OH \longrightarrow CH_3CHO \text{ (acetaldehyde)} + H_2 \quad (1)$$

$$2\ CH_3CHO \longrightarrow CH_3C\text{-}O_2C_2H_5 \text{ (ethylacetate)} \quad (2)$$

$$CH_3CHO + 2\ C_2H_5OH \longrightarrow CH_3CH\ (O\ C_2H_5)_2 \text{ (acetal)} \quad (3)$$

$$CH_3CHO + HCHO \longrightarrow CH_3CO_2CH_3 \text{ (methylacetate)} \quad (4)$$

Mixed acetals are formed in a manner similar to acetal except that another alcohol is substituted for ethanol.

The g.c. trace for a sample of the aqueous layer from the cold trap is shown in Figure 2; no attempt was made to optimize the g.c. analysis. Of interest for this study was to identify the peaks at retention times 3.13 and 5.75 minutes. The i.r. spectrum for the compound eluting at 3.13 is shown in Figure 3 (bottom) together with the spectrum for a sample of ethyl acetate (top). The agreement between the two spectra is excellent and identifies the compound responsible for the 3.13 peak as ethylacetate. Likewise, the infrared spectrum of diethylacetal (Figure 4, top) and the peak eluting at 5.47 minutes (Figure 4, bottom) clearly confirm that the peak eluting at 5.47 is acetal.

An ion current g.c.-m.s. spectrum is shown in Figure 5; note that the spectrum starts at 8 minutes. The fragmentation spectrum in Figure 6a agrees with a published electron impact (EI) spectrum for ethyl acetate. Likewise, the mass spectrum shown in Figure 6b corresponds to the Figure 5 peak eluting at 15.1 minutes and agrees with published data for acetal. Several of the minor peaks were also identified by the m.s. EI spectrum: 11.6 minute retention time was 1-methyoxy-1-ethyoxyethane (Figure 6c); 12.6 minute retention time was n-butanol (Figure 6d) and 18.3 minute retention time was ethylbutyrate (Figure 6e).

Acetaldehyde eluted so quickly that it was not amenable to identification by either g.c.-m.s. or g.c.-i.r. without much extra effort. Hence, this compound was identified by confirming its retention time by doping a Fischer-Tropsch sample with an authentic sample of acetaldehyde.

DISCUSSION

Analytical limitations prevented Emmett and coworkers from making a detailed analysis of the oxygenates in their ^{14}C tracer studies. The introduction of gas chromatographic analysis allowed for more detailed analysis of the products as, for example, was done by one of the pioneers, Pichler, of Fischer-Tropsch synthesis (14). Included in reference 14 was an analysis for C_1 through C_5 alcohols but other oxygenates were not indicated by the g.c. for alcohols produced by a promoted Co catalyst while reference 11 presents analysis of oxygenates formed using an iron catalyst.

The oxygenates produced in the current study are readily identified if they are derived from the added ^{14}C labeled alcohol. A number of these oxygenates have been identified by g.c.-m.s. and/or g.c.-i.r. The use of g.c.-i.r. is in its infancy and the quality of the i.r. spectra, combined with the high resolution capability of capillary g.c. and the unique quantitative capabilities of g.c. and i.r., point toward rapidly expanding usage of this technique. In Fischer-Tropsch studies, the qualitative and quantitative application for analysis for alkenes, alcohol or carbonyl compounds in peaks comprised of coeluting compounds should make this an important analytical procedure.

The presence of acetaldehyde is not surprising since aldehydes and ketones have been previously reported. The data in Figure 7 show that ethanol and acetaldehyde are at, or near, equilibrium concentrations for the conditions utilized for this run. THe ratio of ethanol/acetaldehyde is essentially the same when the reactant feed is CO/H_2/ethanol or when the ethanol feed is replaced by an approximately equimolar mixture of ethanol and acetaldehyde (Figure 7). Thus, dehydrogenation of the ethanol added as a ^{14}C labeled

reactant to acetaldehyde (reaction 1) readily accounts for the presence of acetaldehyde. The ethanol and acetaldehyde have essentially the same specific activity (Table 1) as is required for a rapidly equilibrating mixture of these two compounds.

It is surprising that ethanol and acetaldehyde readily undergo conversion in the present case. Carbon monoxide is present in a much higher concentration than ethanol in the reactant mixture (CO:ethanol = 47:3 molar ratio). There is extensive evidence to show that CO is chemisorbed on metals that function as methanation on Fischer-Tropsch catalysts by the formation of a metal carbon bond, not a metal oxygen bond. This implies that the metal-carbon bond is more stable under synthesis conditions than a metal-oxygen bond is; presumably this would be true even for those conditions where CO dissociation occurs. If this premise is accepted it is difficult to see how ethanol, where the carbonyl carbon is saturated with bonds to two hydrogen atoms and a methyl group in addition to the hydroxyl oxygen, could dominate in a competition with CO for surface sites. Moreover, i.r. evidence suggests that alcohols are adsorbed to form a metal-oxygen bond (15-18). Why can an alcohol more readily compete for metal sites by bonding through a metal-oxygen bond when CO avoids this metal-oxygen bond to form instead a metal-carbon bond? The current experiments were carried out with the catalyst particles dispersed into an octacosane solvent. Surface adsorption should then be determined by the concentration of dissolved gases, CO and ethanol. There is evidence to support the view that ethanol accumulates by some mechanism in the reactor to a much higher concentration than its concentration in the reactant mixture entering the reactor. Unfortunately, we do not know, at this time, the extent that CO accumulates above its fraction in the feed. If, as seems reasonable, CO does not accumulate to nearly the extent that

ethanol does, relative concentration of these two reactants could provide an answer to the above question. Thus, the CO:ethanol mole ration of 47:3 for the feed gas would be a much greater than the ratio in the liquid phase; this relative concentration could increase by ethanol absorption over that expected from the gas phase composition. This could then explain the rapid conversion of ethanol; and the dramatic decrease in CO conversion when ethanol is added to the syngas feed. Kinetic studies of Fischer-Tropsch synthesis with iron catalysts in slurry phase are available (for example, see 19-21); however, these, as well as those for fixed bed reactions, usually include CO, H_2 and water but ignore alcohols and other oxygenates. Vedage and Klier (22) did compare the competitive hydrogenation of CO, hydrocarbons and oxygenates for a Cu/ZnO methanol synthesis catalyst and found that the same active sites were involved in the hydrogenation of aromatics, olefins, carboxylic acids, aldehydes and carbon monoxide. While there may be little, if any, direct evidence to support the proposal of build-up of ethanol and aldehyde concentrations in slurry phase reactors with iron catalysts, this concept does explain the current data and is, by analogy, consistent with results obtained with other catalyst systems.

For homogeneous catalytic systems, the synthesis of a series of low molecular weight alcohols and esters is readily accomplished (23-27). For example, Knifton et al. (28) found that, for a series of ruthenium bimetallic catalysts, alcohol carbonylation of methanol provided a reaction pathways to produce acetic acid and ethanol. In the present study, however, the pathway to ethylacetate formation cannot be through carbonylation. First, while more methanol is formed when ethanol was added than when it was absent, the amount of ethylacetate exceeds by a factor of 10 the total methanol plus methylacetate formed when syngas only was used as a feed. Secondly, and more

convincing, is that the relative ^{14}C activity of ethylacetate is essentially twice that of ethanol. Methanol and CO present when ^{14}C labeled ethanol was added to the feed does not contain a detectable level of ^{14}C. Thus any acetic acid formed from methanol and CO is, at our detection level, unlabeled. Even if this unlabeled acetic acid reacted with ^{14}C labeled ethanol, the relative activity of the ester would be 1 rather than the 1.9 observed experimentally. This means that the predominate quantity of both the acid and alcohol used in forming the ester must have come from the added alcohol. This presents a problem since ethanol or, more likely, acetaldehyde must be oxidized to acetic acid, or at least a precursor, even though the system contains approximately 3 atm of hydrogen (ca. 0.4 to 0.6 relative pressure) that should overall, provide a reducing, rather than oxidizing condition. The Cannizzaro reaction provides a mechanism for disproportionation of an aldehyde to equal quantities of an acid and an alcohol; however, this mechanism is limited to aldehydes without -hydrogens so it is not expected to be applicable in the present case. It therefore appears that CO must be involved in the acid formation and, in the present case, it must be as an oxidant, not as a carbonylation species. One means of accomplishing this is to have CO dissociation to form adsorbed carbon and adsorbed oxygen atoms. A significant fraction of the adsorbed oxygen atoms, rather than undergoing hydrogenation to water as usually occurs, react with adsorbed acetaldehyde to form acetic acid. What is proposed here is just a specific example of iron oxidation by CO followed by reduction by the aldehyde. Subsequent reaction of acetic acid with ethanol should be rapid at these reaction temperatures.

Acetal is another major product. Its formation is easily accounted for using well known organic reactions:

$$CH_3CHO + C_2H_5OH \longrightarrow CH_3CH(OH)(OC_2H_5) \longrightarrow CH_3CH(OC_2H_5)_2$$

An analogue of acetal, with a methal group substituted for one ethyl group, is formed in about half the quantity of acetal. The hemiacetal, if present, is at a much lower concentration than acetal and was not identified.

Aldol condensation of acetaldehyde followed by dehydration and alkene function hydrogenation produces butyraldehyde; the presence of a larger quantity of ethyl butanoate than of ethyl propanoate is indicative of a minor amount of product being formed by aldol condensation.

The presence of small amounts of ^{14}C containing normal alcohols with three or more carbons suggests that either a small amount of ethanol undergoes carbonylation with subsequent reduction and/or chain initiation by ethanol followed by growth and a termination step that produces an alcohol. The present data does not permit us to discriminate between these two possibilities. Likewise, 5 to 15% of the added ^{14}C appears to be incorporated into hydrocarbons; a discussion of this aspect of the synthesis is beyond the scope of this paper.

In summary, ethanol undergoes conversion to a number of oxygenates during syngas conversion with an iron catalyst. The reactions involved are summarized in the scheme outlined below where the major products are enclosed in boxes and minor product pathways are indicated by broken arrows.

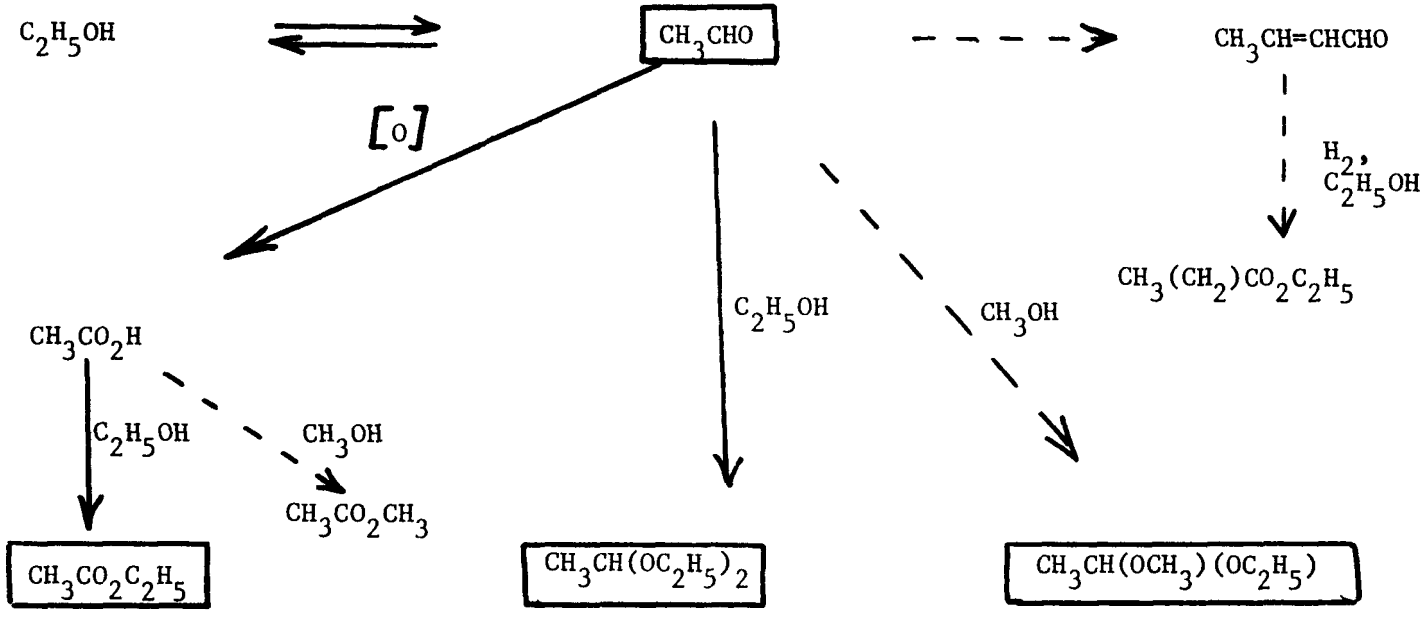
C2H5OH
CH3CHO
CH3CH=CHCHO
[O]
H2,
C2H5OH
CH3(CH2)CO2C2H5
CH3CO2H
C2H5OH
CH3OH
C2H5OH
CH3OH
CH3CO2CH3
CH3CO2C2H5
CH3CH(OC2H5)2
CH3CH(OCH3)(OC2H5)

Table 1

Oxygenated Compounds Formed From Syngas Alone and When ^{14}C Labeled Ethanol was Added

Compound	Reaction Mixture		Relative Radioactivity
	CO/H_2	$CO/H_2/C_2H_5OH$	^{14}C/mole[a]
Alcohols			
CH_3OH (methanol)	0.373	0.912	
C_2H_5OH (ethanol)	0.536	12.6	1.0
C_3H_7OH (1-propanol)	0.210	0.293	b
C_4H_9OH (1-butanol)	0.038	0.067	b
$C_5H_{11}OH$ (1-pentanol)	0.01		
Aldehydes			
CH_3CHO (acetaldehyde)	0.07	1.27	1.09
Esters			
$CH_3CO_2CH_3$(methylacetate)	---	0.40	0.94
$CH_3CO_2C_2H_5$ (ethylacetate)	---	6.11	1.93
Acetals			
$CH_3CH(OC_2H_5)_2$ (acetal)	---	0.134	b
$CH_3CH(OCH_3)(OC_2H_5)$		0.084	b
$CH_3CH(OCH_3)$		0.050	b
$CH_3CH(OC_2H_5)(OC_3H_7)$		0.025	b

a. Activity relative to ethanol = 1.0.

b. Small amounts of compound and/or absence of reliable thermal conductivity response factor allows only approximate relative activity determinations.

In preparations to develop reliable procedures to carry out ^{14}C labeled studies, a 100 day run was carried out in a slurry reactor (1 liter) that contained 130 grams of a 9.2% Fe on silica catalyst. Reaction conditions were such that we obtained approximately 20% CO conversion. Under these reaction conditions, the conversion remained essentially constant during the 100 days (Figure 8). The selectivity, based on C_3 hydrocarbon in the gas phase (excluding CO, H_2 and CO_2), remained constant throughout the run. Thus, these low conversion levels this umpromoted, silica supported catalyst retained its activity during 100 days of nearly continuous operation.

There are several possibilities to consider when ^{14}C labeled ethanol feed is introduced into the CO/H_2 syngas feed to effect a step change in feed concentrations. The flow scheme for the reactor and sample collection system is shown schematically in Figure 9. In operation the 1 liter autoclave reactor is approximately half full of solvent; thus, the gas volume is approximately 1/2 liter. The combined volume of the two product traps is approximately 600cc. The volume of the connecting tubing is negligible in comparison to that of the reactor and product traps.

Figure 10 can be used to define the flow situation for several senerios. In Figure 10 I and P symbolize intermediate compound(s) and products, respectively, that are derived from ^{14}C labeled ethanol.

We consider first the simplest case (I) where the concentration of ^{14}C ethanol in the solvent is negligible compared to the flow rate of ethanol into and out of the reactor. Thus, the concentration of ethanol in the reactor gas volume, and hence in the product stream, should attain equilibrium in 5 to 6 time constants that are based on the reactor gas volume. With a gas flow rate of about 300cc/min. the effluent stream will contain 99% or greater of the ^{14}C ethanol concentration in the feed streams (Figure 11 where is the time

of EtOH on stream and is the mean resident time). The same curve applies for any ^{14}C alcohol provided we express alcohol feed in moles with respect to the CO/H_2 syngas feed. This calculation assumes that ethanol is well-mixed with the CO/H_2; this should be the case. The less than 20 minutes to attain a steady state ^{14}C ethanol concentration in the reactor effluent stream will be unaffected by reaction provided the assumption of insignificant ethanol in the solvent applies; with such a reaction condition the concentration of ethanol in the effluent stream after 20 minutes will be at steady state with a concentration reduced from that in the feed stream in proportion to the fraction that undergoes conversion.

The data in Figure 12 show that the concentration of ethanol in the effluent stream does not attain a steady state until about 5 or more hours after initiating alcohol feed. Likewise, aldehyde product concentration in the product stream increases during a 10 hour period. The data in Figure 12 is clearly inconsistent with the assumptions involved in case I.

One could argue that the data in Figure 12 is an artifact introduced by the reactor system as, for example, holdup in the product traps. The data presented in Figure 13 show that this should not be the the case. Ethanol concentration in the effluent stream should decline when ethanol feed is terminated in a manner consistent with the increase in Figure 12. Both product traps containing ^{14}C labeled materials are removed and replaced by empty traps at the same time the ethanol feed is terminated; hence, any material in the effluent stream cannot come from the traps. The data for the gas effluent stream for 24 hours after terminating ethanol flow are presented in Figure 13. This Figure 13 data is entirely consistent with that in Figure 12 since steady-state is not attained even after 8 hours. A third set of data (Figure 14) is also consistent with ethanol concentrating in the solvent so

that the assumptions for case I do not apply. When ethanol is added to the syngas the propane/propene ratio is altered (Figure 14); there is a gradual decrease in the propane/propene ratio that parallels the build-up in EtOH concentration in the effluent gas stream. In addition there is a gradual increase in the propane/propene ratio after the termination of ethanol feed (Figure 14). Finally, the radioactivity appearing in the effluent gas stream at increasing time, starting when the introduction of ethanol began, is shown in Figure 15. While the ^{14}C activity curve shows a less gradual ethanol increase in ^{14}C content than Figure 12, it agrees with approximately 9 hours, rather than ca. 20 minutes, being required to attain steady-state effluent gas ^{14}C ethanol concentration. In considering the data in Figures 12-15 it should be realized that we are constructing them with data collected for other reasons since we did not anticipate the hold-up problem and, consequently, did not design sample collection specifically for this purpose.

The other extreme (case II) would be for k_1, to be very large, and the ratio k_{-1}/k_1 to be very small so that, within the 1 to 3 day time scale used for ^{14}C labeled alcohol addition studies, essentially all of the added alcohol would remain in the reactor. The data clearly eliminate this extreme (case II) does not apply.

The actual situation for alcohol addition lies somewhere between these two extreme cases. Thus, the alcohol added initially must dissolve very rapidly in the octacosane solvent. Within about 8 hours the solvent becomes saturated with ethanol so that $k_1[p_{EtOH}] = k_{-1}(EtOH)$, where the rate constants are defined in Figure 10, P_{EtOH} is the partial pressure of ethanol in the gas phase and (EtOH) is the molar concentration of ethanol in the solution. It is not clear at this time whether an intermediate, I, also acts to provide a reservoir of ethanol in the solvent phase during the period following the

termination of alcohol addition in the syngas feed. The oxygenates identified thus far provide one scheme whereby intermediates could be an effective means of providing such ethanol storage:

$$C_2H_5OH \rightleftharpoons CH_3CHO$$

$$CH_3CHO + 2EtOH \rightleftharpoons CH_3CH(OC_2H_5)_2$$

Acetal formation, with a much higher boiling point then ethanol, provides a reaction pathway that would retard the attainment of the steady-state ethanol concentration in the effluent gas. Likewise, the reverse reaction, decomposition of acetal, provides an ethanol source following termination of the ethanol feed. While we cannot rule out intermediate formation, the influence of pentanol and decanol upon the propane/propene ratio, as described earlier in this report, show that alcohol accumulation probably plays a role. When we take liquid sample directly from the reactor during the next run we will be able to answer this question.

The retention of pentanol and decanol follow the expected trend; that is, it takes longer to attain the steady-state ^{14}C pentanol concentration in the effluent gas that it does for ^{14}C ethanol. In turn, it takes longer with decanol than with pentanol. However, we did not obtain sufficient data to completely define the time-concentration curves for these two reactants during this run, but will do during the next run.

The implications of these results are for reaching. The higher molecular weight products produced in a CSTR would be determined to a great extent, if not entirely, by secondary reactions. With porous catalysts, condensation of oil and waxes on and in the catalyst would cause similar, if not as dramatic, effects.

The data shown in Figure 16 is consistent with retention of higher boiling components. Hydrogenation of olefins, as a secondary reaction, can occur when under our reaction conditions. The data in Figure 16 shows that the fraction of alkane comprising each n-alkane plus n-alkene carbon number fraction increases with increasing carbon number. Very little olefin is observed for C_{16} and higher carbon number materials. The amount of 2-alkene in the 2-alkene plus 1-alkene fraction decreases with increasing carbon number (Figure 17). Based upon the thermodynamic data for C_4 and C_7 alkenes, we anticipate between 1-alkene to comprise about 10 to 20% of the 1-alkene plus 2-alkene fraction. For C_7-C_9, it appears that the 1-alkene concentration is nearly the equilibrium value. However, as the carbon number increases the 1-alkene comprises a larger fraction of the 1-alkene plus 2-alkene components. This is not expected is isomerization to equilibrium occurs with carbon number due to larger retention in the reactor. This expectation neglects (1) that internal olefins are frequently hydrogenated at a more rapid rate and (2) some component, as yet unidentified, coelutes with the 1-alkene and the fraction of this unidentified component increases with increasing carbon number. These possibilities will be investigated using g.c.-m.s. and g.c.-i.r. as well as ^{14}C labeled alkenes added during the course of the studies with the alkali promoted catalyst.

REFERENCES

1. J. T. Kummer, T. W. DeWitt and P. H. Emmett, J. Amer. Chem. Soc., 70, 3632 (1948).

2. W. K. Hall, R. J. Kokes and P. H. Emmett, J. Amer. Chem. Soc., 79, 2983 (1957).

3. J. T. Kummer, and P. H. Emmett, J. Amer. Chem. Soc., 73, 2886 (1951).

4. W. K. Hall, R. J. Kokes and P. H. Emmett, J. Amer. Chem. Soc., 82, 1077 (1960).

5. J. T. Kummer and P. H. Emmett, J. Amer. Chem. Soc., 75, 5177 (1953).

6. R. J. Kokes, W. K. Hall and P. H. Emmett, J. Amer. Chem. Soc., 79, 2989 (1957).

7. G. Blyholder and P. H. Emmett, J. Phys. Chem., 64, 470 (1960).

8. G. Blyholder and P. H. Emmett, J. Phys. Chem., 63,, 962 (1959).

9. H. Pichler and H. Schulz, Chem. Ing. Tech., 42, 1162 (1970).

10. H. Schulz and H. D. Achtsnit, Rev. Portuguesa Quin. (Lisboa), 19, 317 (1977).

11. H. Schulz and A. Zeinel Deen, Fuel Proc. Tech., 1, 31, 45 (1977).

12. H. Schulz , B. Rao and M. Elstner, Erdzas Kohle-Erdgas-Petrochem., 30, 651 (1970).

13. H. Schulz, Erdol u Kohle-Erdgas-Petrochemie, 30, 123 (1977).

14. H. Pichler, H. Schulz and M. Elstner, Brennstoff-Chemie, 48, 78 (1967).

15. G. Blyholder and L. D. Neff, J. Phys. Chem., 70, 893, 1738 (1966).

16. G. Blyholder and D. Shihabi, Proc. Int. Congr. Catal., 6th, 1976, Vol. 1, p. 440 (1977).

17. G. Blyholder, D. Shihabi, W. V. Wyatt, and R. Bartlett, J. Catal., 43, 122.

18. G. Blyholder and W. V. Wyatt, J. Phys. Chem., 70, 1745 (1966).

19. H. Nettelhoff, R. Kokuun, S. Ledakowicz and W. D. Deckwer, German Chem. Eng., 8, 177 (1985).

20. H. E. Atwood and C. O. Bennett, Ind. Eng. Chem., Process Des. Dev., 18, 163 (1979).

21. J. L. Feimer, P. L. Silveston and R. R. Hudgins, Ind. Eng. Chem., Product Res. & Dev., 20, 609 (1981).

22. G. Vedage and K. Klier, J. Catal., 77, 558 (1982).

23. M. Pijolat and V. Perrichan, Appl. Catal., 13, 321 (1985).

24. W. Keim, M. Berger and J. Schlupp, J. Catal., 61, 359 (1980).

25. F. G. A. van den Berg and J. H. E. Glezer, Proc. Koninklijke Nederlandse Akademie Wentschappen, Ser. B., 86, 227 (1983).

26. L. C. Costa, Catal. Rev. Sci. Eng., 25, 325 (1983).

27. D. R. Fahey, J. Amer. Chem. Soc., 103, 136 (1981).

28. J. F. Knifton, R. A. Grigsby, Jr. and J. J. Lin, Organometallics, 3, 62 (1984).

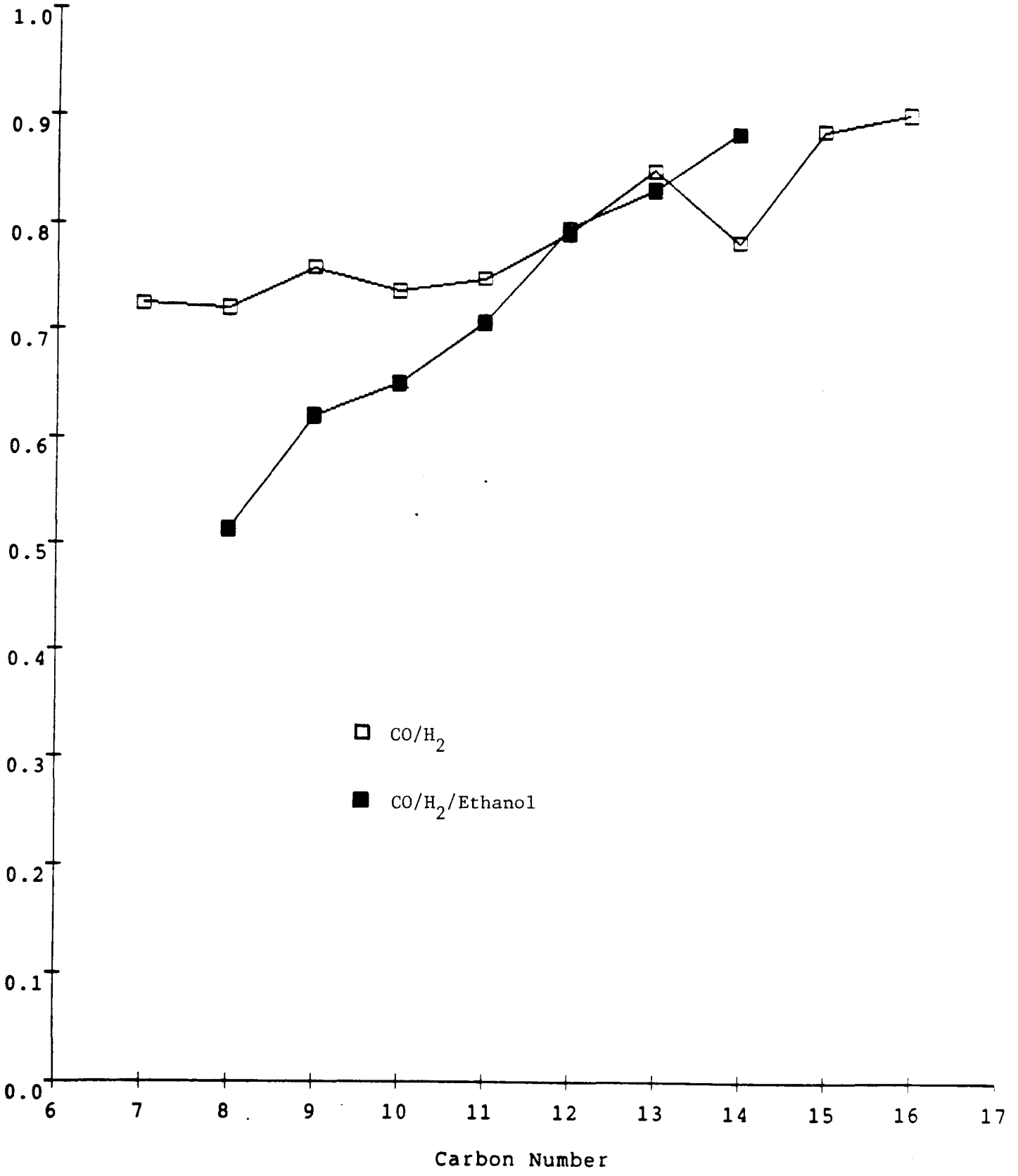

Figure 1. Fraction of n-alkane, based upon n-alkane plus n-alkenes, for each of the above carbon numbers for syngas only ( ) and for syngas plus ethanol ( ) (the C_{14} peaks for syngas only contains a minor amount of another component and is lower than if a correction is made for this impority component).

Figure 2. Capillary g.c. trace for an aqueous layer of the cold trap; the peaks correspond to the g.c.-i.r. spectra shown in the following figures.

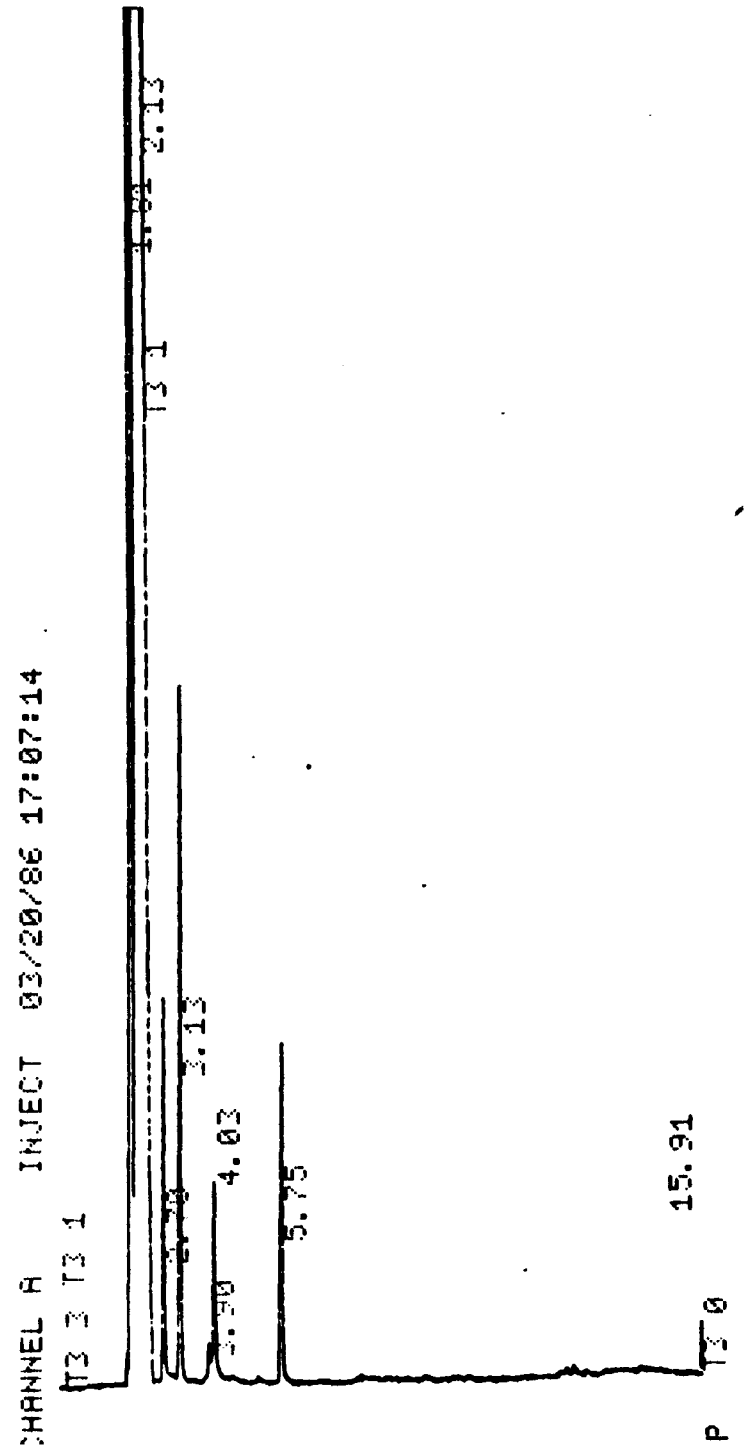

Figure 3. Ethyl acetate spectrum (top) and the g.c.-i.r. spectrum (bottom) of the peak eluting at 3.13 minutes in figure 2.

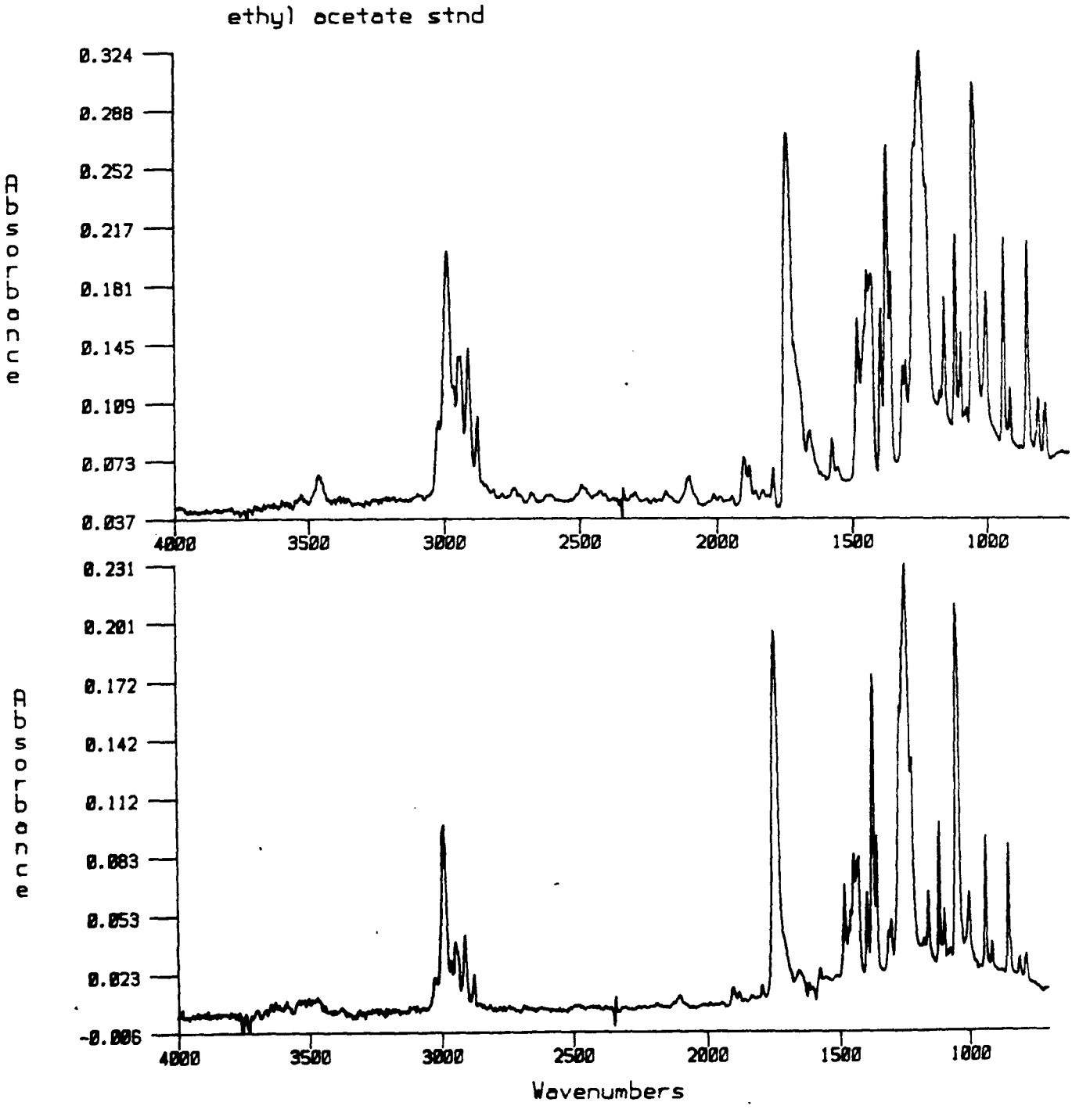

Figure 4. Acetal spectrum (top) and the g.c.-i.r. spectrum (bottom) for the peak eluting at 5.47 minutes in figure 2.

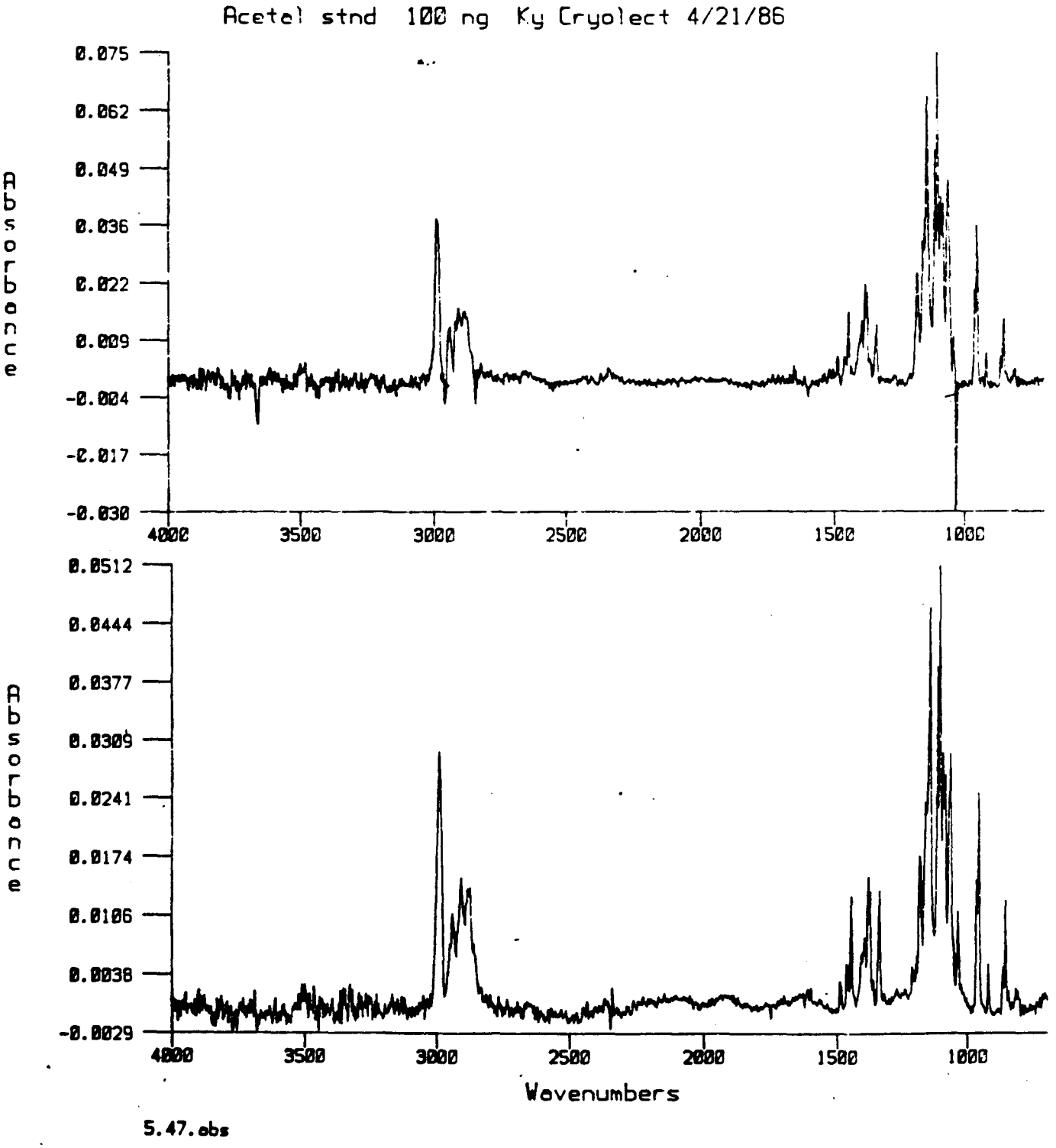

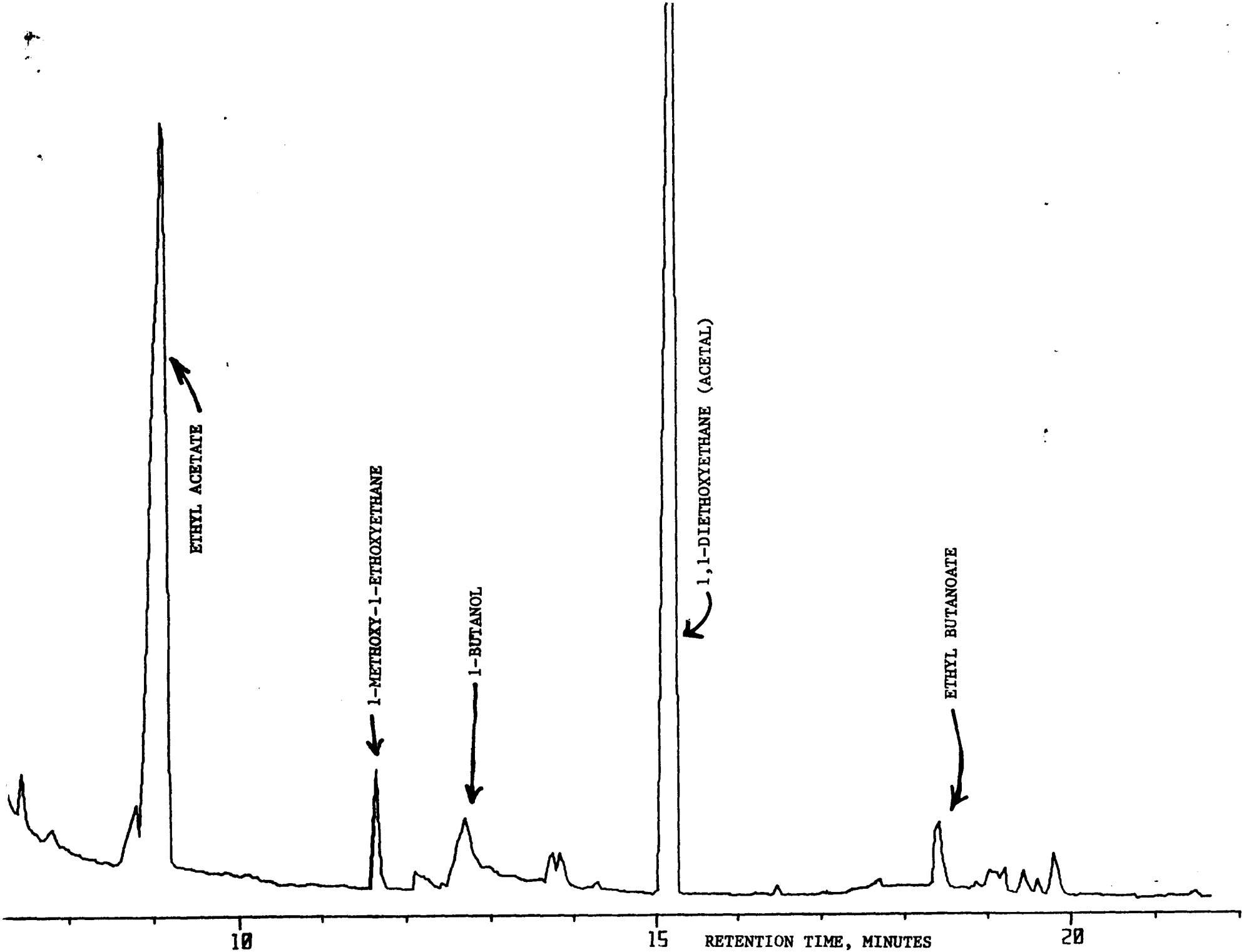

Figure 5. G.c.-m.s. ion current trace for an aqueous layer from the cold trap.

Figure 6a. Electron impact (EI) spectrum for the peak eluting at about 9 minutes in figure 5. (spectrum agrees with published one for ethyl acetate).

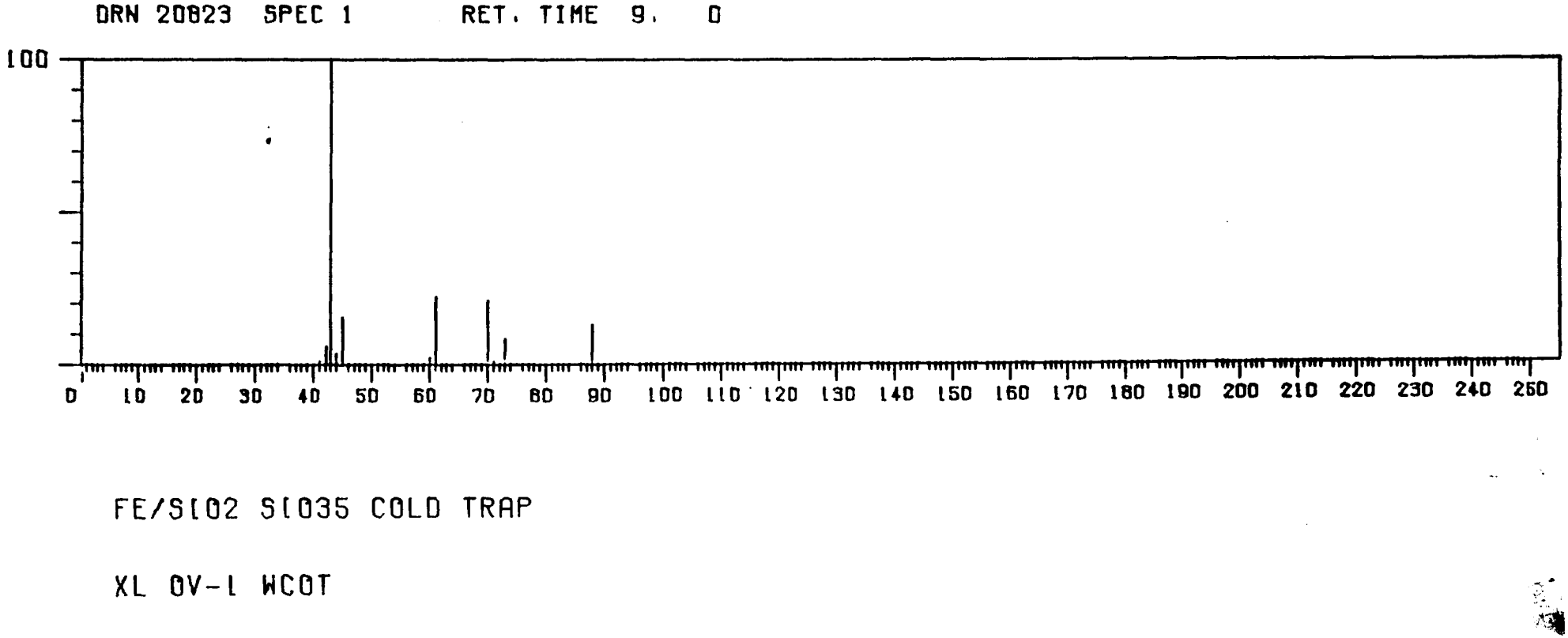

Figure 6b. Electron impact (EI) spectrum for the peak eluting at about 15.1 minutes in figure 5 (spectrum agrees with published one for acetal).

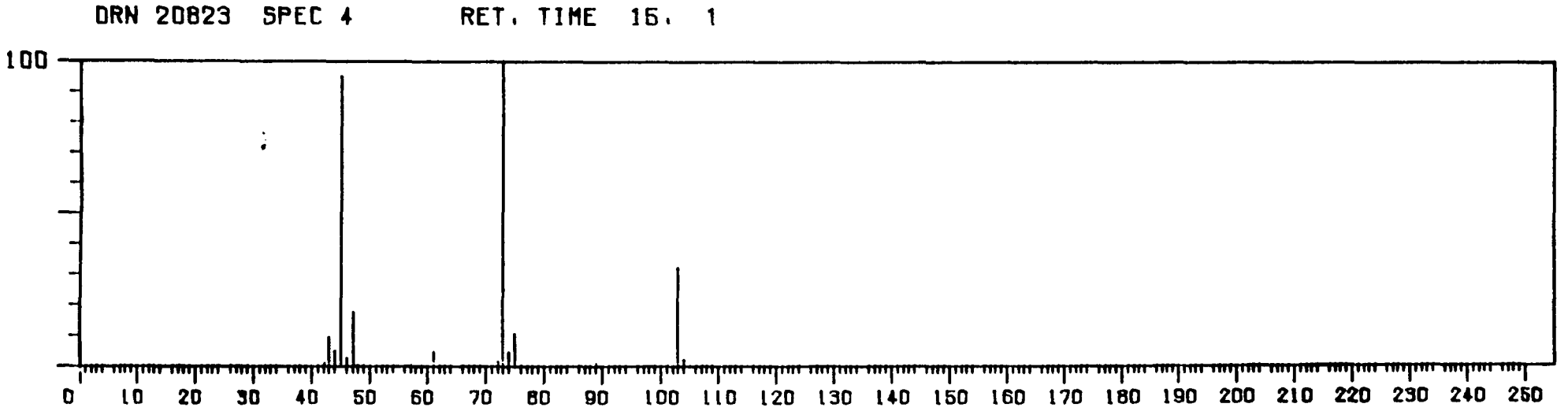

Figure 6c. Electron impact (EI) spectrum for the peak eluting at about 11.6 minutes in figure 5 (spectrum agrees with published one for 1-methoxy-1-ethoxyethane).

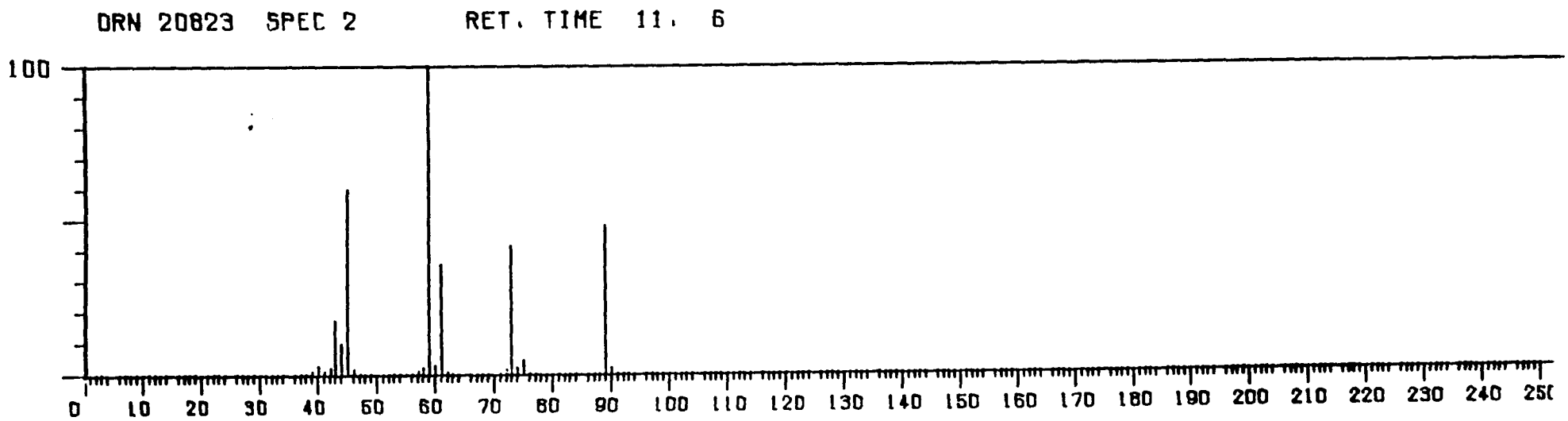

Figure 6d. Electron impact (EI) spectrum for the peak eluting at about 12.6 minutes in figure 5 (spectrum agrees with published one for n-butanol).

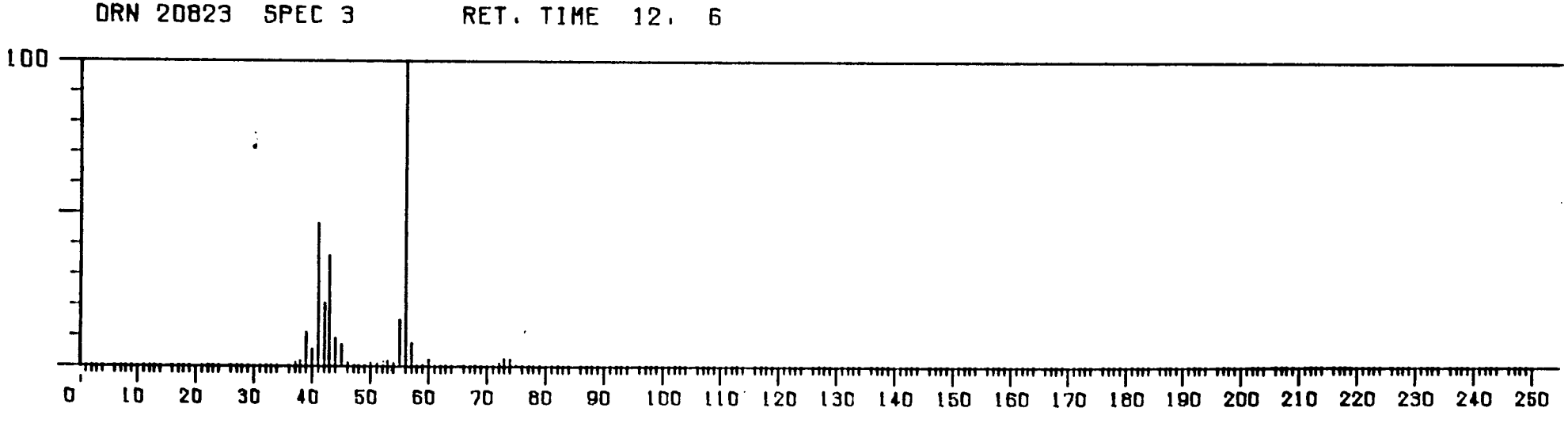

Figure 6e. Electron impact (EI) spectrum for the peak eluting at about 18.3 minutes in figure 5 (spectrum agrees with published one for ethylbutanoate).

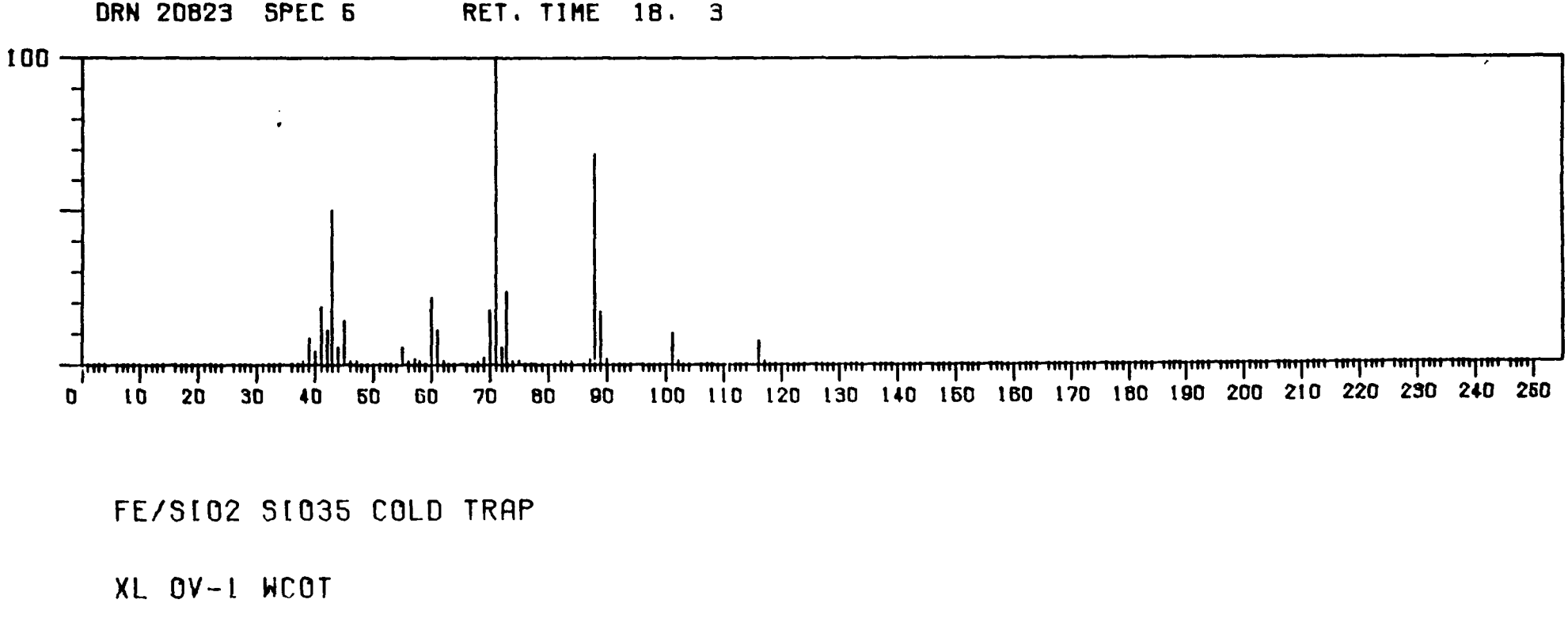

Figure 7. Plot showing that similar ethanol/acetaldehyde ratios are obtained when the syngas feed contains only ethanol (○) or an equal molar mixture of ethanol and acetaldehyde (△).

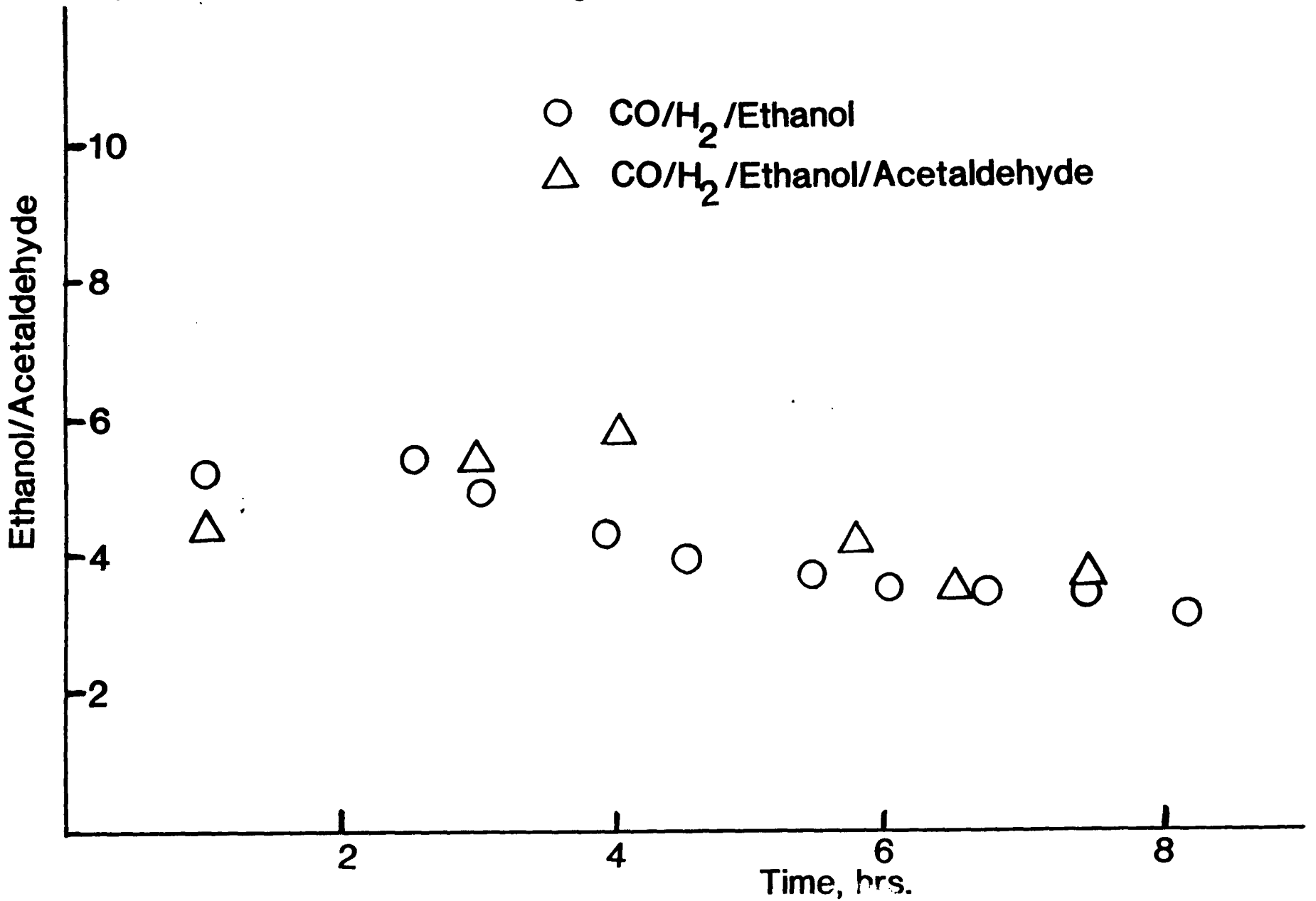

Figure 8. Plot showing that the conversion, based on CO, is essentially constant during a 100 day run with Fe/SiO_2 catalyst and the constant amount of C_3 hydrocarbon in the gas phase indicating essentially constant selectivity.

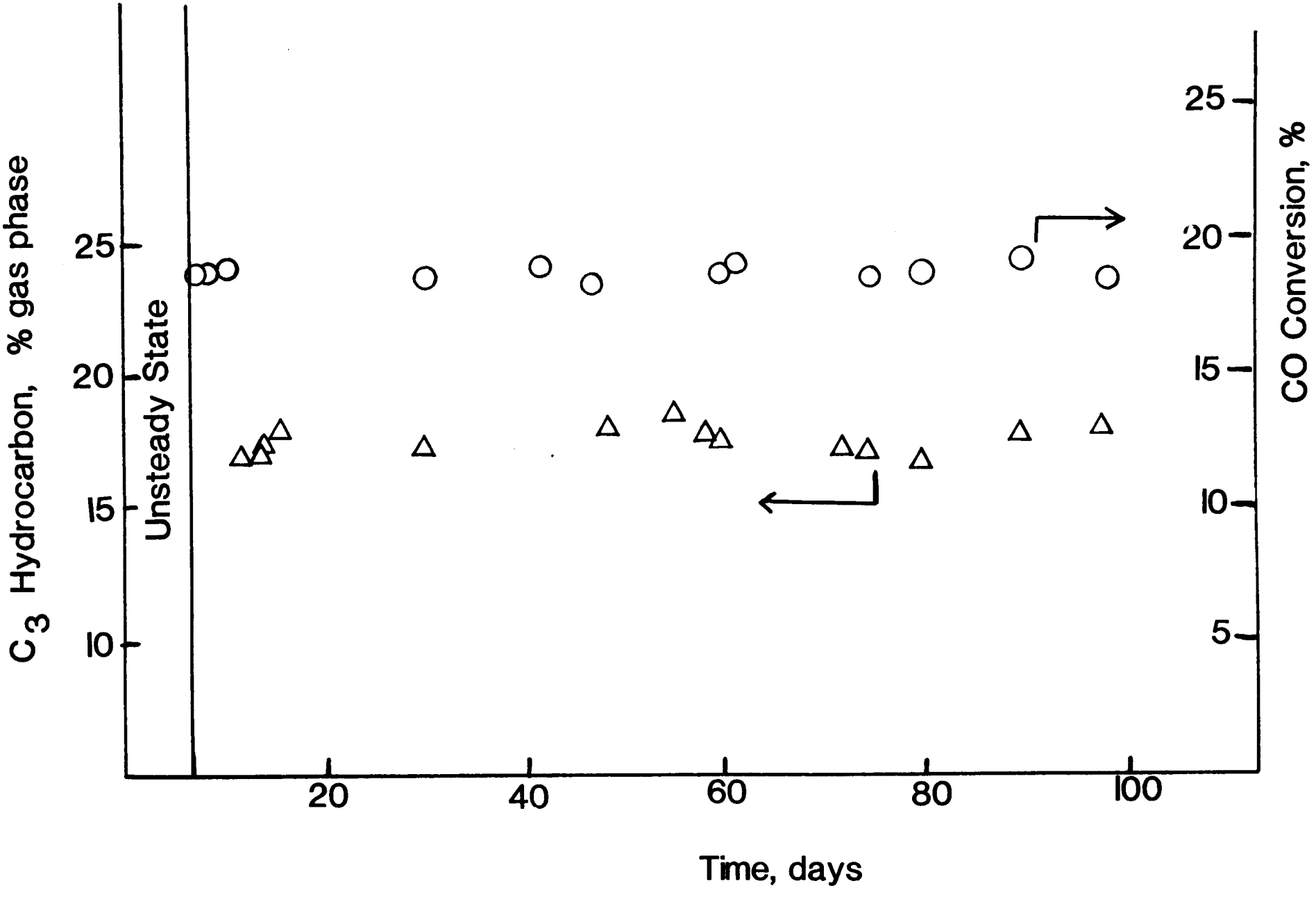

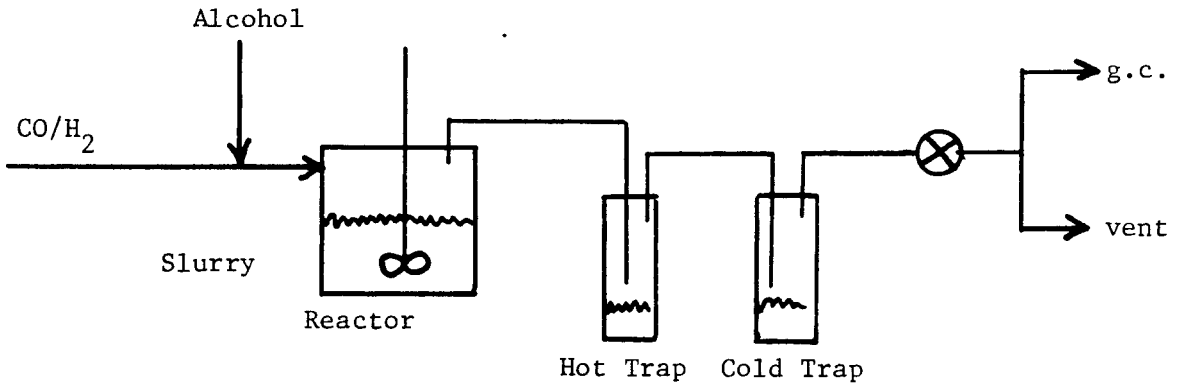

Figure 9. Schematic of Fischer-Tropsch reactor system.

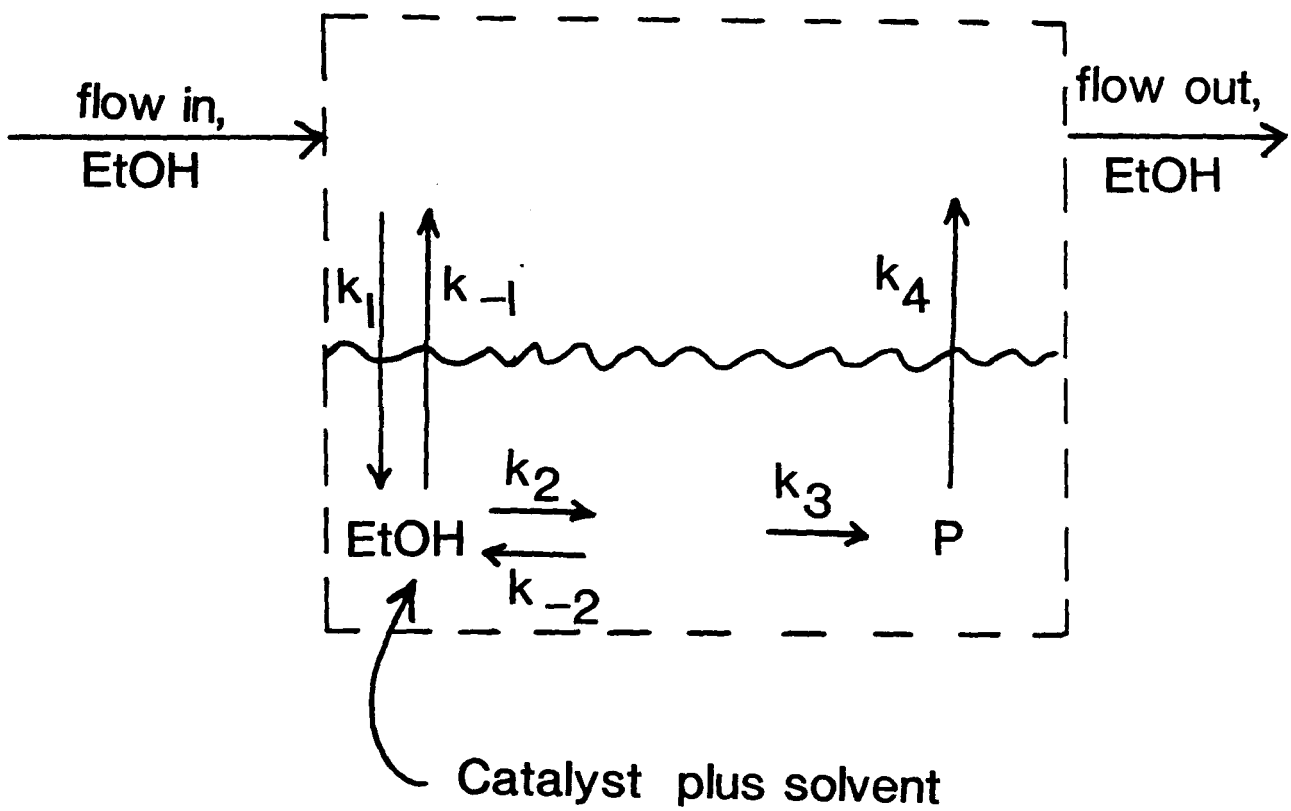

Figure 10. Schematic of the possible ethanol flow and hold-up for the reactor only.

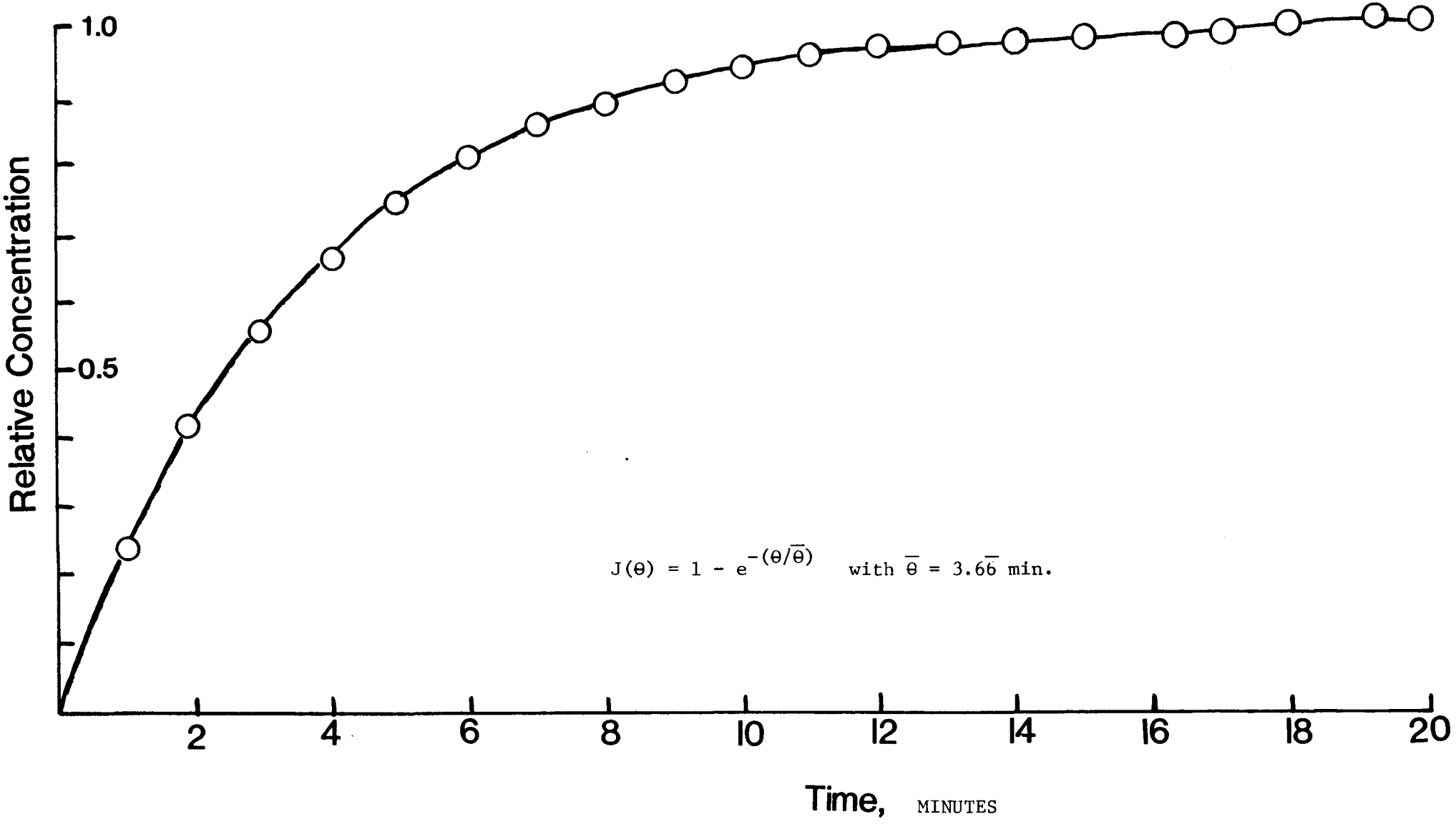

Figure 11. Calculated relative concentration of ethanol in the effluent gas stream, with ethanol addition initiated in the feed stream at time zero, based upon 500 ml gas phase and perfect mixing of ethanol and syngas.

Figure 12. Experimentally measured effluent gas ase concentration of ethanol(○) and acetaldehyde (△) (ethanol addition to the feed gas was initiated at time = 0 in the above scale; also not that time in figure 11 is expressed in minutes but in hours in this figure).

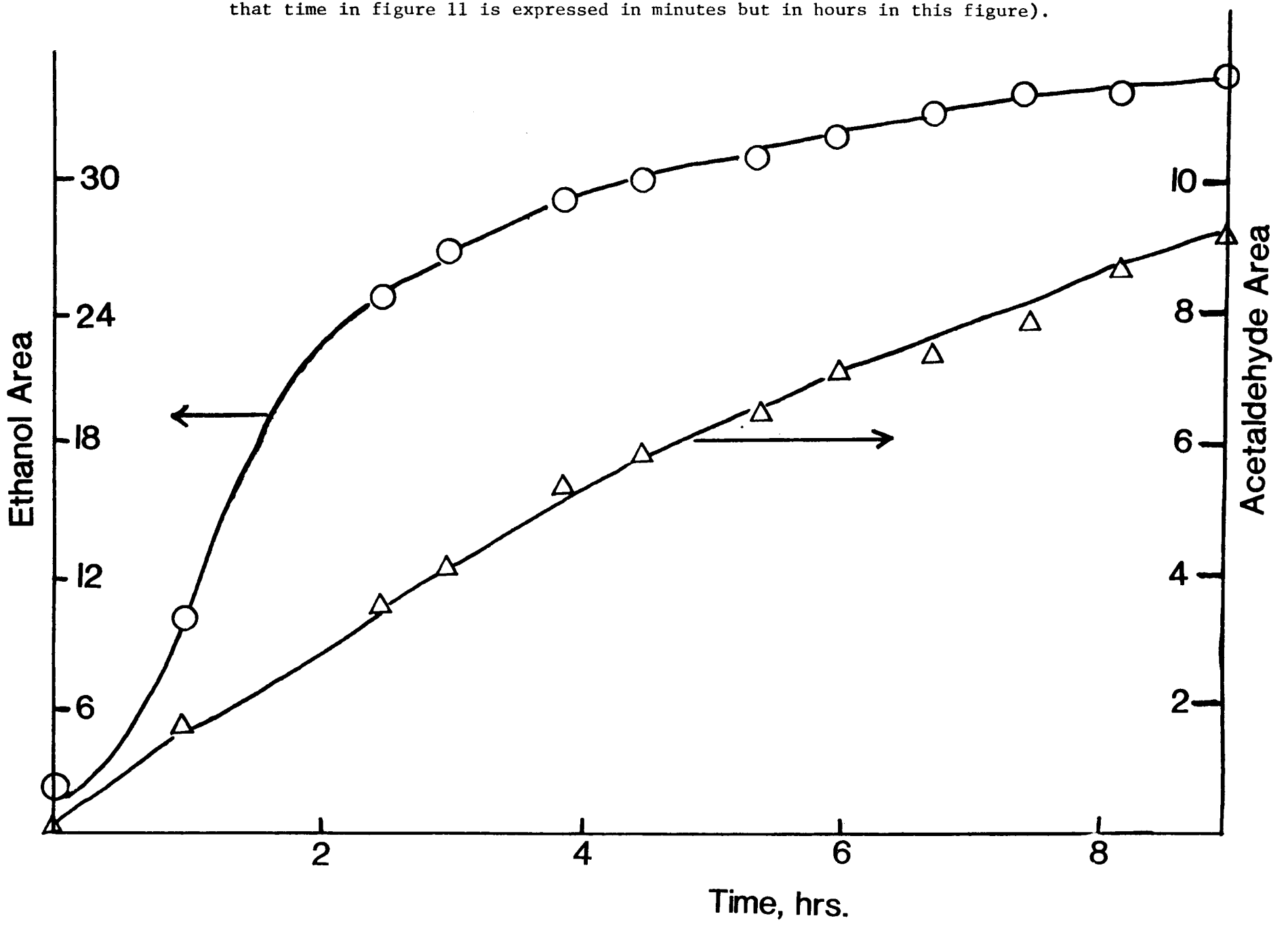

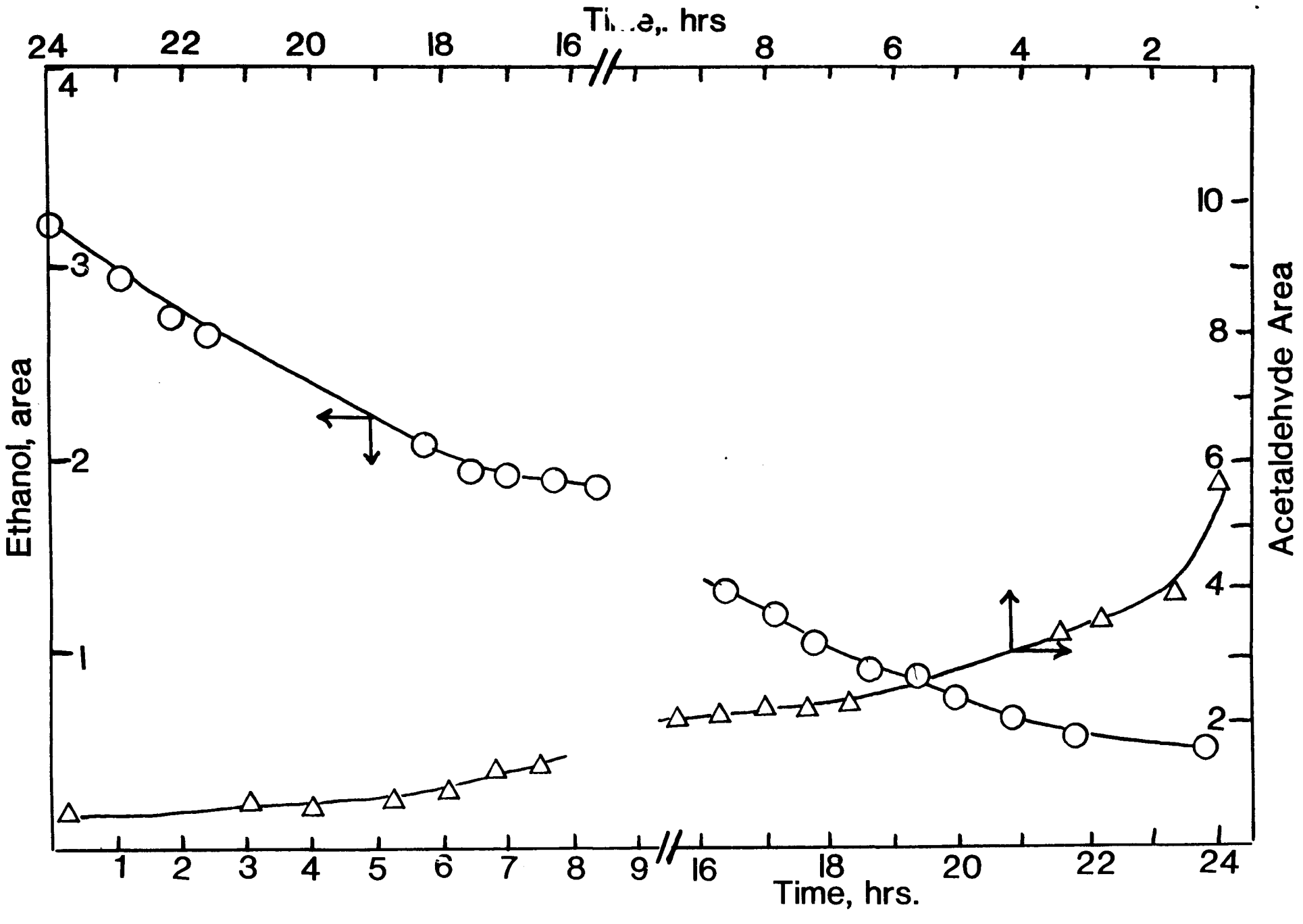

Figure 13. Concentration of ethanol and acetaldehyde in the effluent gas stream after terminating ethanol addition to the feed stream at time zero on the time scale of the above figure.

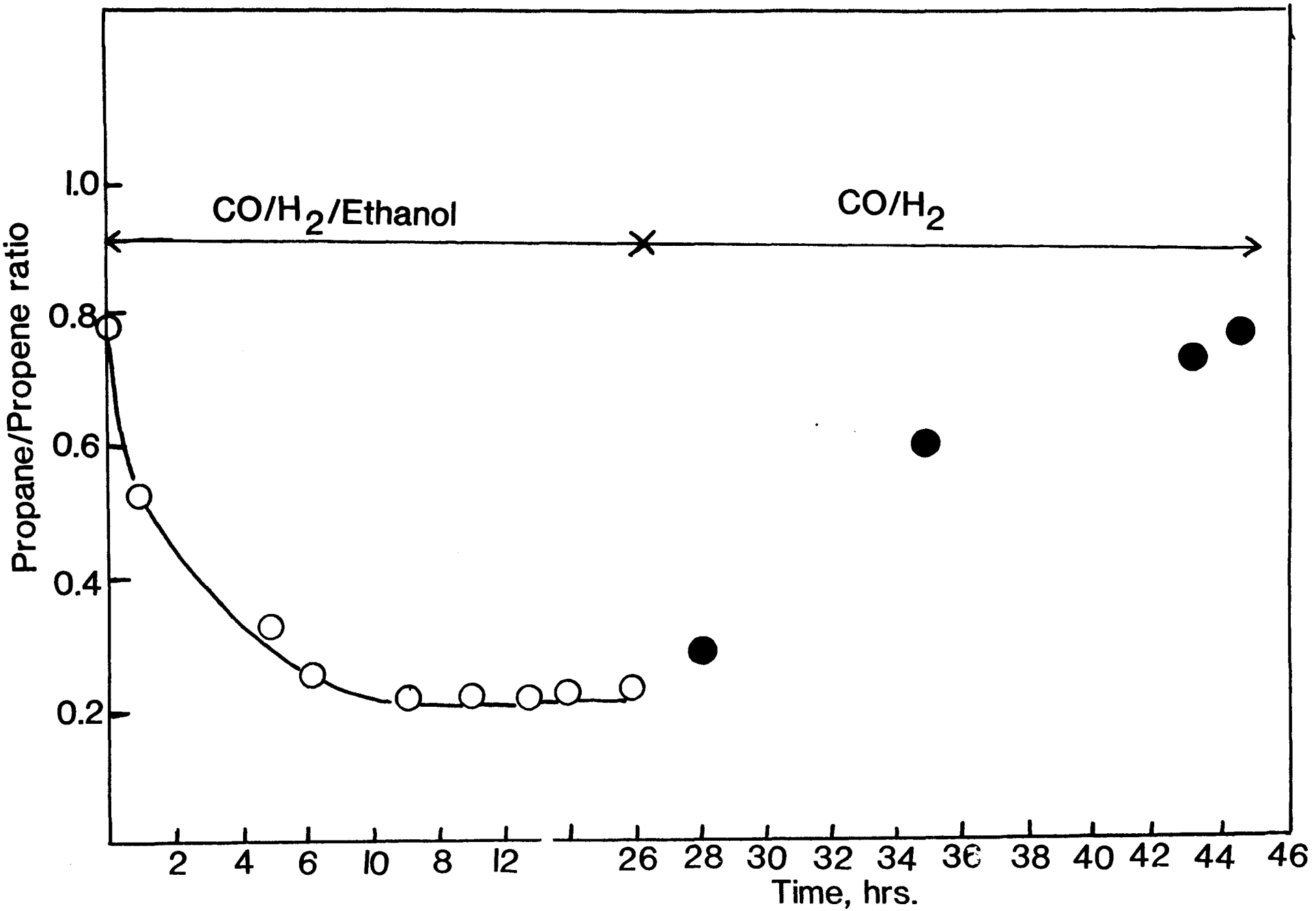

Figure 14. Propane to propene ratio in the gas stream following ethanol addition to the syngas feed stream at time zero and terminating the ethanol addition at 26 hours in the above figure.

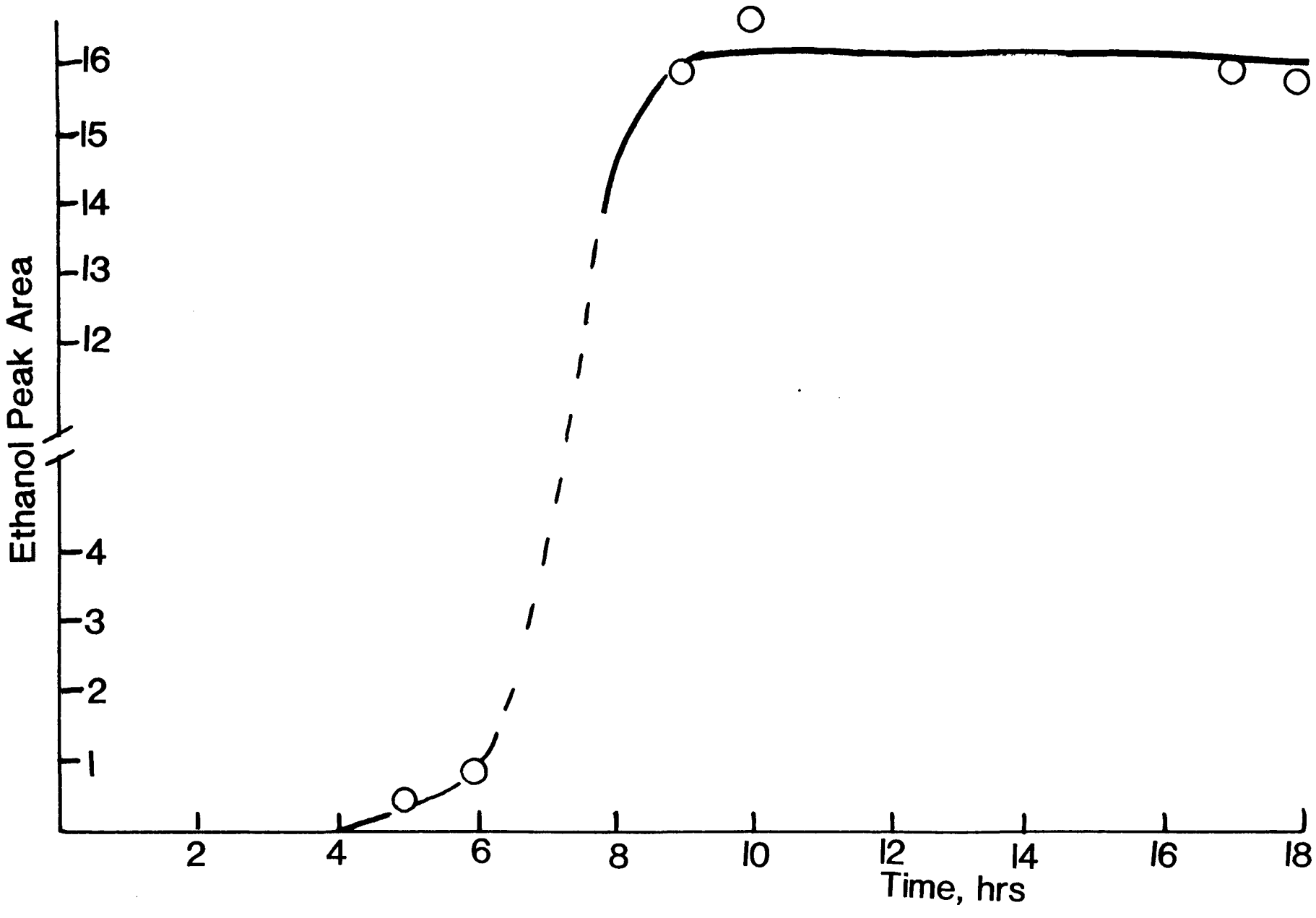

Figure 15. Relative peak area corresponding to the ^{14}C content of ethanol in the effluent gas stream (^{14}C labeled ethanol added to the feed gas stream at time zero).

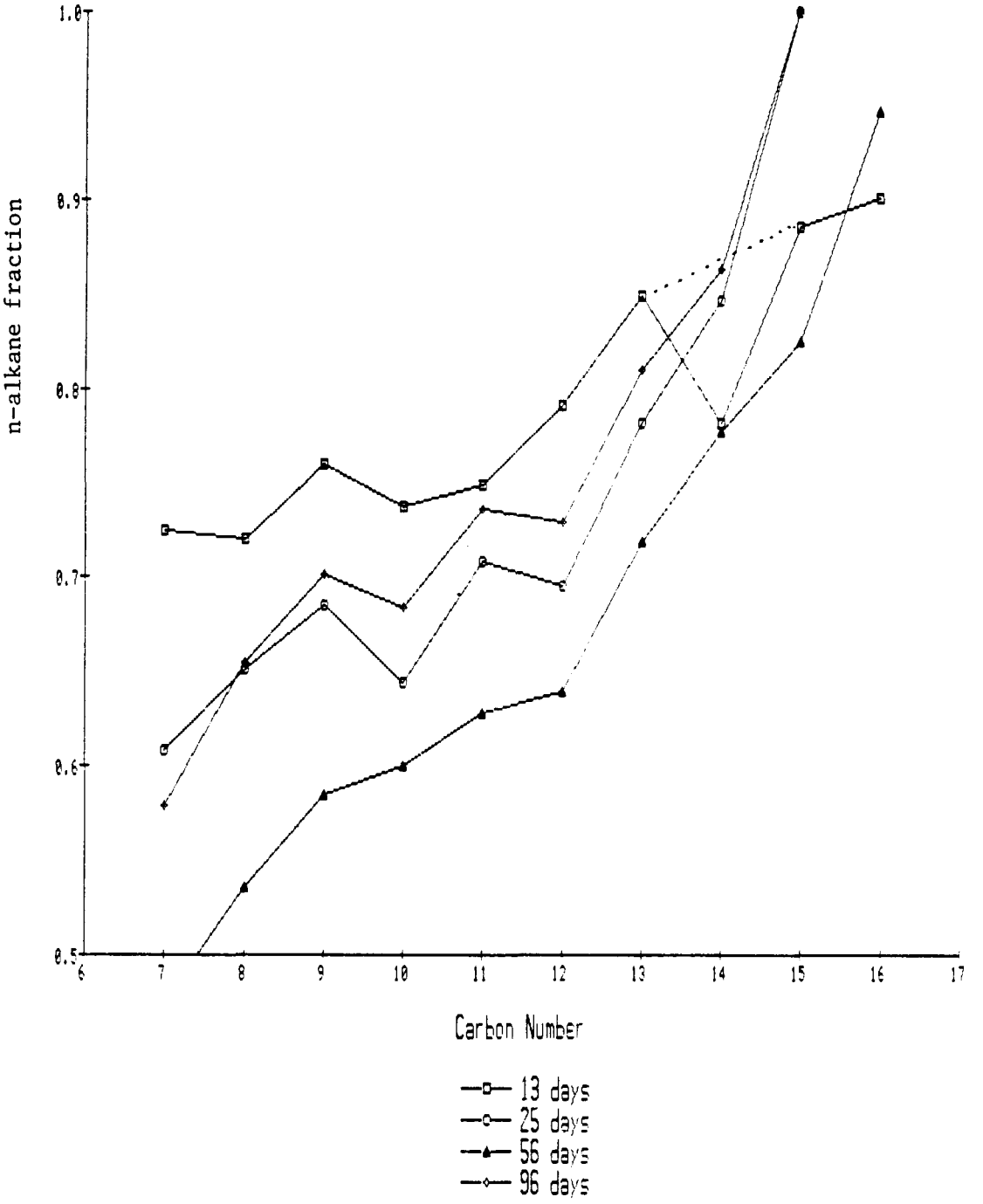

Figure 16. The fraction of n-alkane, based on n-alkane plus n-alkenes, for C_7 to C_{16} carbon number for increasing days of catalyst use.

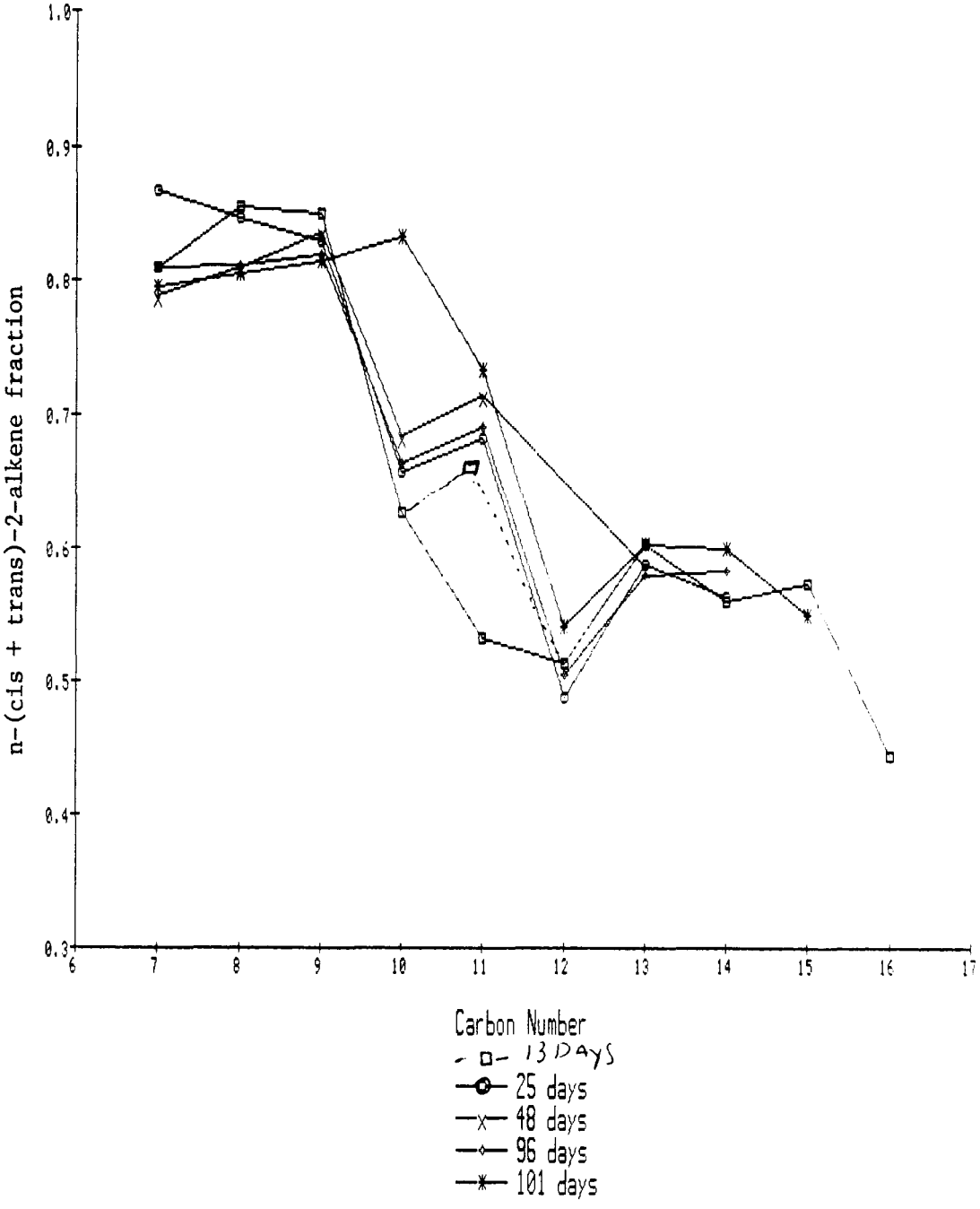

Figure 17. The fraction n-(cis + plus)-2-alkene, based on total n-alkene, for increasing carbon number during increasing catalyst age.